OSBORNE, N. S. & GINNINGS, D. C. (1947). *J. Res. Natl. Bur. Stand.* **39**, 453–477.
PROSEN, E. J., JOHNSON, W. H. & ROSSINI, F. D. (1946). *J. Res. Natl. Bur. Stand.* **36**, 455–461.
RIHANI, D. N. & DONAISWAMY, L. K. (1965). *Ind. Eng. Chem.* pp. 17–21.
RITCHIE, J. P. (1988). *Tetrahedron*, **44**, 7465–7478.
SCOTT, D. W., GUTHRIE, G. B., MESSERLY, J. F., TODD, S. S., BERG, W. T., HOSSENLOP, I. A. & MCCULLOUGH, J. P. (1962). *J. Phys. Chem.* **66**, 911–914.
SILVA, M. A. V. DA & MONTE, M. J. S. (1992). *J. Chem. Thermodyn.* **24**, 715–724.
SMITH, J. A. S., WEHRLE, B., AGUILAR-PARRILLA, F., LIMBACH, H. H., FOCES-FOCES, C., CANO, F. H., ELGUERO, J., BALDY, P., PIERROT, M., KHURSID, M. M. T. & LACOMBE-MCDOUALL, J. R. (1989). *J. Am. Chem. Soc.* **111**, 7304–7312.
STEWART, J. M., MACHIN, P. A., DICKINSON, C. W., AMMON, H. L., HECK, H. & FLACK, H. (1976). *X-ray System of Crystallographic Programs*. Technical Report TR-446. Computer Science Center, Univ. of Maryland, College Park, Maryland, USA.

Acta Cryst. (1994). B**50**, 762–771

Structures with Identical Packing; Racemic and Partially Optically Pure 3-(2′-Chloro-2′-phenylethyl)-2-thiazolidiniminium *p*-Toluenesulfonate and a Comparison of the Packing in Corresponding Racemic and Optically Active Compounds

BY KATALIN MARTHI AND SINE LARSEN

Centre for Crystallographic Studies, Department of Chemistry, University of Copenhagen, Universitetsparken 5, *DK*-2100 *Copenhagen, Denmark*

AND MÁRIA ÁCS,* JÓZSEF BÁLINT AND ELEMÉR FOGASSY

Department of Organic Chemical Technology, Technical University of Budapest, PO Box 91, *H*-1521 *Budapest, Hungary*

(*Received* 7 *February* 1994; *accepted* 28 *April* 1994)

Abstract

The crystal structures have been determined for racemic and two optically active samples of 3-(2′-chloro-2′-phenylethyl)-2-thiazolidiniminium *p*-toluenesulfonate ($C_{11}H_{14}ClN_2S^+.C_7H_7O_3S^-$) from low-temperature (122 K) X-ray diffraction data. The three crystal structures are virtually identical. The racemate crystallizes in the space group $P2_1/n$, $Z = 4$, with unit-cell dimensions $a = 8.5016\ (10)$, $b = 8.2803\ (11)$, $c = 27.447\ (3)$ Å and $\beta = 96.478\ (9)°$. The cation displays disorder of the Cl atom and the C atom to which it is bonded. The disorder can be rationalized in terms of the presence of two partially populated enantiomers with different conformations. The two optically active salts contain both enantiomers of the chiral cation. The ratios between the *R*- and *S*-enantiomers were estimated to be 0.944 (7)/0.056 (7) and 0.860 (7)/0.140 (7). Both salts crystallize in the space group $P2_1$ with unit-cell dimensions almost identical to those of the racemate. The two independent anions and the ring systems of the cations are related by pseudoinversion symmetry. One of the independent cations has a disorder similar to that found for the racemate. The system of hydrogen bonds connecting two cations and two anions into 12-membered rings is identical in the racemic and in the optically active crystals. Additional evidence for the formation of a solid solution between the enantiomers and the racemate is provided by thermoanalytical and IR measurements. The crystal structures of 64 pairs of racemate and its corresponding enantiomer have been analysed. Relations similar to that observed for the salts in the present study were found for six of the pairs. For another eight pairs, there is a great resemblance between the packing of the racemate and the corresponding enantiomers.

Introduction

One of the most effective anthelmintic agents is 6-phenyl-2,3,5,6-tetrahydroimidazo[2,1-*b*]thiazole. Hydrochlorides of the racemate and the *S*-enantiomer are used as drugs and marked under the names *Tetramisole* and *Levamisole*, respectively (Negwer, 1978). The *S*-enantiomer is several times more potent but no more toxic than the *R*-isomer and is the one used to treat humans. The activity of

* Deceased.

this drug is closely related to its chirality. We are investigating the absolute configuration of the different reaction intermediates in a selected synthetic route of *Levamisole* and *Tetramisole* (Hungarian Patent 203108, 1991, Japanese Patent 62-238293, 1987), as the synthetic route involves several steps where inversion or racemization of the chiral center is possible. 3-(2′-Chloro-2′-phenylethyl)-2-thiazolidinimine shown below is one of the reaction intermediates. We undertook structure determinations of the *p*-toluenesulfonic acid salts of the racemate and what was thought to be an almost pure enantiomer of the base. To our surprise, both enantiomers of the base were found in the optically active salt, which has its crystal packing identical to the racemic salt. This prompted a structural study of the *p*-toluenesulfonate salt of a more optically pure sample of 3-(2′-chloro-2′-phenylethyl)-2-thiazolidinimine.

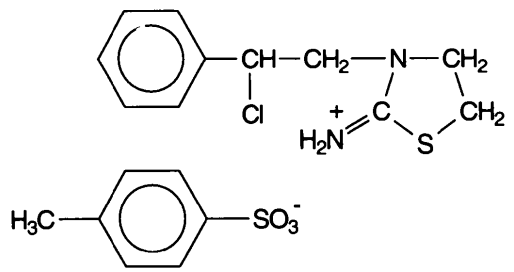

We report here the results from these structure determinations of 3-(2′-chloro-2′-phenylethyl)-2-thiazolidiniminium *p*-toluenesulfonate that have different optical purities of the base (RAC, OA72 and OA89). The similarity between the crystal packing in these three compounds initiated a survey of the relations between the structures of corresponding racemic and enantiomeric compounds. The analysis was primarily based on the structures extracted by Brock, Schweitzer & Dunitz (1991) from the Cambridge Structural Database (Allen, Kennard & Taylor, 1983), and the results from this investigation are presented.

Experimental

Spectroscopic measurements

Optical rotations at 589 nm (Na_D) were measured on a Perkin–Elmer 241 polarimeter at room temperature.

IR spectra between 4000 and 400 cm^{-1}, with a spectral resolution of 4 cm^{-1}, were measured on KBr pellets with an ITS-7 spectrometer.

Thermodynamic measurements

Melting points were measured by differential scanning calorimetry (DSC) using a PL–DSC instrument calibrated with indium and tin. The measurements were carried out with a heating rate of 5° min^{-1} on samples in hermetically closed crucibles. The mass of the samples was in the range 3.0–4.5 mg. Possible decomposition of the compounds was examined by thermogravimetric measurements with a PL–TGA-1000 instrument.

Preparations

Samples of 3-(2-chloro-2′-phenylethyl)-2-thiazolidiniminium chloride with different optical purities were prepared by the method described by Spicer *et al.* (1968), slightly modified for the optically active compounds (Hungarian Patent 203108, 1991). Attempts to obtain good crystals of the hydrochloride salts were futile. Instead they were converted to salts of *p*-toluenesulfonic acid by direct reaction. By recrystallization of the *p*-toluenesulfonates from methanol, crystals suitable for X-ray diffraction investigations could be obtained, although recrystallization never enhanced the optical purity.

Racemic 3-(2′-chloro-2′-phenylethyl)-2-thiazolidiniminium *p*-toluenesulfonate (RAC) crystallizes as white needles. A similar crystal habit was observed for what was expected to be a salt of the pure enantiomer, which had optical rotation $[\alpha]_D = -25.2$ ($c = 1$, methanol; OA72). However, the crystal-structure determination revealed that both enantiomers are present in this crystal. From the optical rotation and the ratio between the two enantiomers in the crystal of OA72, we estimated the maximum optical rotation to be 35 ($c = 1$, methanol) for the optically pure salt. However, the structure determination on a crystal from what we thought was an optically pure salt (OA89) ($[\alpha]_D = -37$ {$c = 1$, methanol}) revealed that it contains the *R*- and *S*-enantiomers in the ratio 0.944 (7)/0.056 (7).

X-ray diffraction

Weissenberg photographs showed that all three crystals RAC, OA72 and OA89 belong to the monoclinic system. The systematically absent reflections $h0l$, $h + l = 2n + 1$ and $0k0$, $k = 2n + 1$ were found for the racemic salt (RAC), which uniquely determine its space group to be $P2_1/n$. The diffraction patterns recorded for the two optically active crystals OA72 and OA89 were very similar to that observed for the racemic compound (RAC). The $0k0$ reflections were systematically absent for $k = 2n + 1$, later checked with ψ-scans on the diffractometer. In addition, it was observed that the $h0l$ reflections with $h + l$ odd were systematically weaker than those where $h + l$ were even. A subsequent analysis of the reflections measured with the diffractometer showed that 40% of the $h0l$ reflections with $h + l$ odd have

Table 1. *Crystals data and summary of the data collection and structure refinement results*

	RAC	OA72	OA89
Formula	$C_{11}H_{14}ClN_2S^+.C_7H_7O_3S^-$	$C_{11}H_{14}ClN_2S^+.C_7H_7O_3S^-$	$C_{11}H_{14}ClN_2S^+.C_7H_7O_3S^-$
Formula weight	412.94	412.94	412.94
Radiation	Cu $K\alpha$ (λ = 1.54184 Å)	Cu $K\alpha$ (λ = 1.54184 Å)	Cu $K\alpha$ (λ = 1.54184 Å)
Temperature (K)	122.0 (5)	122.0 (5)	122.0 (5)
Space group	$P2_1/n$	$P2_1$	$P2_1$
a (Å)	8.5016 (10)	8.533 (3)	8.583 (3)
b (Å)	8.2803 (11)	8.2238 (9)	8.190 (3)
c (Å)	27.447 (3)	27.477 (12)	27.479 (6)
β (°)	96.478 (9)	96.13 (3)	95.70 (2)
V (Å^3)	1919.8 (4)	1917.1 (11)	1922.1 (11)
Z	4	4	4
F(000)	864	864	864
Crystal size (mm)	0.10 × 0.16 × 0.42	0.05 × 0.12 × 0.40	0.03 × 0.13 × 0.38
D_x (g cm^{-3})	1.429	1.431	1.427
μ (Cu $K\alpha$) (mm^{-1})	3.973	3.979	3.969
Reflections used in determination of cell parameters	22	16	15
θ range (°)	38.42–42.74	28.78–34.19	21.15–40.66
Scan type	ω–2θ	ω–2θ	ω–2θ
$(\sin\theta\lambda^{-1})_{max}$ (Å^{-1})	0.626	0.627	0.626
Standard reflections	110, 21$\bar{1}$, 114	020, 114, 00$\bar{8}$	020, 002, 114
Maximum variation of intensity control reflections (%)	7 (applied)	4 (not applied)	8 (applied)
Range of h	0–10	0–10	0–10
Range of k	0–10	0–10	−10–9
Range of l	−34–34	−34–34	−34–34
R_{int}	0.0115	0.0222	0.0274
Transmission factor range	0.381–0.695	0.320–0.822	0.537–0.888
Number of measured reflections, including standard reflections	4624	4637	5211
Number of independent reflections	3960	4240	4429
Number of observed reflections [$I > 2\sigma(I)$]	3831	3631	4109
w^{-1} ($P = F_o^2 + 2F_c^2$)/3	$\sigma^2(F_o^2) + (0.0314P)^2 + 3.8660P$	$\sigma^2(F_o^2) + (0.0766P)^2$	$\sigma^2(F_o^2) + (0.0810P)^2 + 0.9017P$
Number of variables	254	479	479
R for $F > 4\sigma(F)$	0.0501	0.0595	0.0474
wR_2 for all F^2 data	0.1272	0.1477	0.1317
S for all F^2 data	1.216	1.053	1.033
Max. shift/e.s.d.	−0.001	−0.001	−0.001
Max., min. $\Delta\rho$ (e Å^{-3})	0.71, −0.68	0.46, −1.01	0.40, −0.46
Absolute structure parameter, x	—	0.01 (3)	−0.01 (2)

intensities less than $3\sigma(I)$. The space group of the optically active crystals was determined to be $P2_1$ with two independent salt pairs related by pseudo-inversion symmetry.

The data collections for the three salts (RAC, OA72 and OA89) were performed with a CAD-4 diffractometer. Cu $K\alpha$ radiation (λ = 1.54184 Å) obtained from a graphite monochromator was used. The crystals were cooled with an Enraf–Nonius gas-flow low-temperature device. The temperature, 122 K, was monitored with a thermocouple placed a few centimetres above the crystal in the exhaust pipe. It remained constant within 1 K during the experiments. The different experimental conditions with a summary information of the data reduction and refinement results are presented in Table 1. An analysis of reflection profiles provided the basis for the selection of the scan mode and scan interval for the data collection. The intensities of three standard reflections were measured every 10000 s. The orientation of the crystal was checked after every 300 reflections. The reflections used for intensity control showed systematic variations for RAC and OA89. In the data reduction performed with the *DREADD* data reduction package (Blessing, 1987), corrections were made for these variations, Lorentz, polarization, background and absorption effects. Reflections related by the symmetry of the crystal class were averaged.

The structures were solved by direct methods using *SHELXS*86 (Sheldrick, 1990) and refined by full-matrix least squares, minimizing $\sum w(|F_o^2| - |F_c^2|)^2$ using *SHELXL*93 (Sheldrick, 1995). Scattering factors were taken from *International Tables for Crystallography* (1992, Vol. C) and used as contained in the program. After anisotropic displacement parameters were introduced, the corresponding difference Fourier map showed disorder of the Cl atom in the racemic salt and in one of the cations (labelled *B*) of the optically active salts. The disorder can be described as the presence of two cations of opposite absolute configuration and a different conformation at the same site. This arrangement will lead to two different positions of the Cl atom (Cl*B*) and the C atom (C6*B*) to which the chlorine is bonded. The population parameters of the Cl atoms

were included in the refinements with the constraint that their sum should be 1.00. The two positions of the C atom (C6*B*) to which the Cl is bonded could not be resolved in the optically active crystals OA72 and OA89, although the large displacement parameters of this atom indicate disorder. In the racemic structure RAC, it was possible to describe the two positions of C6*B*. The two atoms C61*B* and C62*B* were given the same population parameters as the Cl atoms to which they are attached.

The refined population parameters can be found in Tables 2 and 3. The difference Fourier maps showed the positions of some of the H atoms. Due to the limited resolution of the data, the positions of the H atoms, except those bonded to the disordered asymmetric C6 atom in OA72 and OA89, were generated according to geometrical and difference electron-density considerations using fixed isotropic displacement parameters. The highest peaks in the final difference Fourier maps were found close to the S atoms. For the optically active crystals, the polar axis restraints were applied according to the method of Flack & Schwarzenbach (1988) and the absolute configuration was established by refinement of the absolute structure parameter x (Flack, 1983). The final value was 0.01 (3) for OA72 and −0.01 (2) for OA89. The structure of OA72 is virtually identical to the structure of the more optically pure salt, OA89; therefore, we have chosen to deposit the structural information on OA72. The final fractional coordinates for RAC and OA89 are listed in Tables 2 and 3.* An inversion twin refinement was performed to check whether the disorder in the optically active salt could be due to twinning, but it resulted in higher R-values.

Table 2. *Atomic coordinates and equivalent isotropic displacement parameters* (Å^2) *for RAC*

$U_{eq} = (1/3)\sum_i —_j U_{ij} a_i^* a_j^* \mathbf{a}_i.\mathbf{a}_j.$

	x	y	z	U_{eq}
S*A*	0.28536 (7)	0.49750 (8)	0.56598 (2)	0.0225 (2)
O1*A*	0.2947 (2)	0.3289 (2)	0.55113 (8)	0.0325 (5)
O2*A*	0.4262 (2)	0.5537 (3)	0.59560 (8)	0.0340 (5)
O3*A*	0.2376 (2)	0.6026 (3)	0.52432 (8)	0.0360 (5)
C1*A*	0.1268 (3)	0.5058 (3)	0.60249 (9)	0.0209 (5)
C2*A*	−0.0221 (3)	0.4521 (3)	0.58303 (10)	0.0248 (5)
C3*A*	−0.1473 (3)	0.4607 (4)	0.61137 (10)	0.0271 (6)
C4*A*	−0.1264 (3)	0.5239 (3)	0.65882 (10)	0.0274 (6)
C5*A*	0.0236 (4)	0.5767 (4)	0.67715 (10)	0.0305 (6)
C6*A*	0.1503 (3)	0.5676 (4)	0.64944 (10)	0.0285 (6)
C7*A*	−0.2609 (4)	0.5344 (4)	0.68980 (12)	0.0392 (7)
S*B*	0.84959 (9)	0.03886 (9)	0.53083 (3)	0.0353 (2)
Cl1*B*[0.821 (3)]*	0.58919 (11)	0.15821 (13)	0.66678 (4)	0.0390 (3)
Cl2*B*[0.179 (3)]*	0.6496 (6)	0.0350 (8)	0.6754 (2)	0.055 (2)
N2*B*	0.6057 (3)	−0.0388 (3)	0.57318 (9)	0.0251 (5)
N15*B*	0.5848 (3)	0.2081 (3)	0.53110 (8)	0.0273 (5)
C1*B*	0.6597 (3)	0.0763 (3)	0.54625 (10)	0.0247 (5)
C3*B*	0.7192 (4)	−0.1676 (4)	0.58958 (14)	0.0401 (8)
C4*B*	0.8481 (4)	−0.1630 (4)	0.55584 (12)	0.0339 (7)
C5*B*	0.4537 (3)	−0.0353 (3)	0.59331 (10)	0.0254 (6)
C61*B*[0.821 (3)]*	0.4691 (5)	−0.0190 (6)	0.64878 (14)	0.0283 (8)
C62*B*[0.179 (3)]*	0.466 (2)	0.062 (2)	0.6388 (6)	0.020 (3)
C7*B*	0.3157 (4)	−0.0021 (4)	0.66983 (11)	0.0361 (7)
C8*B*	0.1879 (4)	0.0894 (4)	0.64834 (12)	0.0368 (7)
C9*B*	0.0486 (4)	0.0950 (4)	0.67020 (14)	0.0428 (8)
C10*B*	0.0375 (4)	0.0140 (5)	0.71329 (13)	0.0454 (9)
C11*B*	0.1631 (5)	−0.0754 (5)	0.73502 (12)	0.0488 (9)
C12*B*	0.3022 (4)	−0.0842 (4)	0.71325 (12)	0.0423 (8)

* Population parameters different from 1.0 are given in square brackets.

Results and discussion

The structure determinations revealed great similarities between the crystal structures of the racemic and the optically active salt. The racemic salt has one ion pair in the asymmetric unit in the space group $P2_1/n$. The optically active salts crystallize in the space group $P2_1$, a subgroup of $P2_1/n$ with two ion pairs in the asymmetric unit which are related by pseudo-inversion symmetry. Summing the x, y and z coordinates of the equivalent atoms in the anion gave values of 0.49, 1 and 0.50. This shows that the equivalent anions are almost related by a pseudo-inversion center close to 0.25, 0.5 and 0.25. It is surprising that the same relationship relates most of the atoms in the chiral cation. The ordered Cl*D* atom is related by this pseudosymmetry to the less populated Cl position in molecule *B*. This pseudosymmetry makes the crystal packing almost identical to that in the racemic salt and explains why the *h*0*l* reflections are systematically weak for $h + l = 2n + 1$.

Descriptions of the cations

Table 4 illustrates the geometry of the cation. Disorder is observed for the cation in the racemate and for one of the cations in the optically active salts. The most disordered fragment of these molecules is the asymmetric C atom and the Cl attached to it. The Cl atom could be resolved in two positions in all three structures, whereas the two positions of the asymmetric C atom could be resolved only in the racemate. However, the rather large displacement parameters for the other atoms bonded to the chiral C atom indicate that they may also be slightly disordered. The disorder of the cation in the racemate corresponds to the presence of both enantiomers at each site in the ratio 0.821 (3):0.179 (3), but as the racemate crystallizes in the centrosymmetric space group $P2_1/n$, this still leads to a racemic crystal. The two enantiomers are not mirror images of each other, since they differ in their relative conformation (Table 4). The torsion angles N2*B*—C5*B*—C61*B*—Cl1*B* [54.5 (3)°] and C8*B*—C7*B*—C61*B*—Cl1*B*

* Lists of structure factors, anisotropic displacement parameters, H-atom parameters, complete geometry and selected torsion angles for OA72 have been deposited at the IUCr (Reference: AB0324). Copies may be obtained through The Managing Editor, International Union of Crystallography, 5 Abbey Square, Chester CH1 2HU, England.

Table 3. *Atomic coordinates and equivalent isotropic displacement parameters* (Å^2) *for OA89*

$U_{eq} = (1/3)\sum_i\sum_j U_{ij}a_i^*a_j^*\mathbf{a}_i.\mathbf{a}_j$.

	x	y	z	U_{eq}
S*A*	0.02638 (11)	0.49480 (13)	0.31514 (3)	0.0226 (2)
O1*A*	0.0352 (4)	0.3238 (4)	0.30031 (12)	0.0324 (8)
O2*A*	0.1640 (3)	0.5478 (5)	0.34548 (12)	0.0349 (8)
O3*A*	−0.0151 (4)	0.6015 (5)	0.27341 (12)	0.0374 (9)
C1*A*	−0.1342 (4)	0.5037 (5)	0.35073 (14)	0.0208 (8)
C2*A*	−0.2783 (5)	0.4397 (6)	0.3317 (2)	0.0249 (9)
C3*A*	−0.4035 (5)	0.4427 (6)	0.3596 (2)	0.0278 (10)
C4*A*	−0.3906 (5)	0.5122 (6)	0.40631 (14)	0.0272 (9)
C5*A*	−0.2467 (5)	0.5769 (7)	0.4238 (2)	0.0318 (11)
C6*A*	−0.1176 (5)	0.5729 (6)	0.3966 (2)	0.0286 (10)
C7*A*	−0.5266 (6)	0.5114 (9)	0.4363 (2)	0.0408 (13)
S*C*	0.45920 (11)	0.50578 (13)	0.18390 (3)	0.0221 (2)
O1*C*	0.4511 (4)	0.6750 (4)	0.19985 (12)	0.0319 (7)
O2*C*	0.3203 (4)	0.4533 (5)	0.15403 (12)	0.0336 (8)
O3*C*	0.5025 (4)	0.3950 (5)	0.22460 (12)	0.0367 (9)
C1*C*	0.6179 (4)	0.4991 (5)	0.14759 (14)	0.0204 (8)
C2*C*	0.7651 (5)	0.5506 (6)	0.16687 (14)	0.0223 (8)
C3*C*	0.8909 (5)	0.5422 (6)	0.1387 (2)	0.0254 (9)
C4*C*	0.8709 (5)	0.4801 (6)	0.0913 (2)	0.0260 (9)
C5*C*	0.7231 (5)	0.4276 (6)	0.0729 (2)	0.0287 (10)
C6*C*	0.5964 (5)	0.4366 (6)	0.1006 (2)	0.0266 (9)
C7*C*	1.0072 (5)	0.4685 (7)	0.0604 (2)	0.0349 (11)
S*B*	0.58081 (13)	0.0318 (2)	0.26978 (5)	0.0348 (3)
Cl1*B*[0.112 (7)]*	0.348 (2)	0.148 (3)	0.4203 (7)	0.074 (10)
Cl2*B*[0.888 (7)]*	0.4054 (2)	0.0251 (3)	0.42537 (5)	0.0492 (7)
N2*B*	0.3552 (4)	−0.0483 (5)	0.31979 (13)	0.0262 (8)
N15*B*	0.3226 (4)	0.2033 (5)	0.27916 (13)	0.0250 (8)
C1*B*	0.4001 (5)	0.0672 (5)	0.29142 (14)	0.0219 (8)
C3*B*	0.4534 (6)	−0.1954 (7)	0.3234 (2)	0.0457 (14)
C4*B*	0.6076 (5)	−0.1525 (8)	0.3062 (2)	0.0362 (11)
C5*B*	0.2102 (5)	−0.0440 (6)	0.34415 (14)	0.0243 (9)
C6*B*	0.2231 (5)	0.0649 (8)	0.3897 (2)	0.0358 (12)
C7*B*	0.0831 (5)	0.0347 (7)	0.4186 (2)	0.0305 (10)
C8*B*	−0.0550 (6)	0.1113 (7)	0.4021 (2)	0.0403 (12)
C9*B*	−0.1877 (7)	0.0937 (8)	0.4264 (2)	0.048 (2)
C10*B*	−0.1819 (7)	−0.0035 (9)	0.4679 (2)	0.048 (2)
C11*B*	−0.0473 (7)	−0.0837 (8)	0.4839 (2)	0.0454 (14)
C12*B*	0.0870 (6)	−0.0647 (7)	0.4597 (2)	0.0390 (12)
S*D*	−0.10257 (13)	0.9643 (2)	0.21639 (4)	0.0304 (3)
Cl*D*	0.16192 (14)	0.8484 (2)	0.08101 (4)	0.0400 (3)
N2*D*	0.1415 (5)	1.0412 (5)	0.17417 (12)	0.0238 (7)
N15*D*	0.1594 (4)	0.7937 (5)	0.21763 (13)	0.0256 (8)
C1*D*	0.0866 (5)	0.9250 (6)	0.20125 (14)	0.0223 (8)
C3*D*	0.0287 (5)	1.1683 (6)	0.1574 (2)	0.0281 (9)
C4*D*	−0.0975 (5)	1.1704 (6)	0.1922 (2)	0.0311 (10)
C5*D*	0.2953 (5)	1.0367 (6)	0.15530 (14)	0.0233 (8)
C6*D*	0.2834 (5)	1.0257 (6)	0.09971 (14)	0.0280 (9)
C7*D*	0.4377 (5)	1.0128 (6)	0.07885 (14)	0.0265 (9)
C8*D*	0.5605 (6)	0.9203 (6)	0.1017 (2)	0.0322 (10)
C9*D*	0.6995 (6)	0.9116 (7)	0.0804 (2)	0.0341 (11)
C10*D*	0.7166 (6)	0.9888 (7)	0.0364 (2)	0.0363 (11)
C11*D*	0.5950 (6)	1.0771 (7)	0.0135 (2)	0.0371 (12)
C12*D*	0.4541 (6)	1.0900 (7)	0.0351 (2)	0.0318 (10)

* Population parameters different from 1.0 are given in square brackets.

[82.1 (4)°] are numerically different from the equivalent angles calculated for the other enantiomer that contains C62*B* and Cl2*B*; the equivalent angles are −38.3 (13) and 154.3 (8)°, respectively.

Fig. 1 shows the relative orientation of the two enantiomers in the crystal. By adopting different conformations, the ring systems of the enantiomers are in identical positions. The optically active salts have one ordered cation (labelled *D*) with the absolute configuration *R*. The other independent cation displays a disorder similar to that observed in the salt of the racemate.

The Newman projections in Fig. 2 and the torsion angles in Table 4 illustrate how the disorder arises from the presence of the cation in different configurations and conformations at the same site. In the RAC structure, the molecular geometry of the more populated conformational isomer of the cation with C61*B* and Cl1*B* is identical to cation *D* or its mirror image in the optically active salt. The cation in the racemate containing the less populated atoms C62*B* and Cl2*B* has a conformation almost identical to the more populated [0.888 (7)] isomer of cation *B* in the optically active salt.

In the optically active salt OA89, a cation with the absolute configuration *R* is found at site *D*, 0.888 (7) of the cations located at *B* also have the absolute

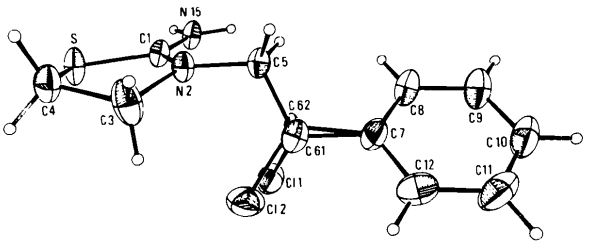

Fig. 1. *ORTEP*II (Johnson, 1976) drawings showing the numbering scheme and the relative orientation of the two enantiomers in the cation of racemic 3-(2′-chloro-2′-phenylethyl)-2-thiazolidiniminium *p*-toluenesulfonate. The thermal ellipsoids are scaled to include 50% probability, H atoms are drawn as spheres with fixed radius.

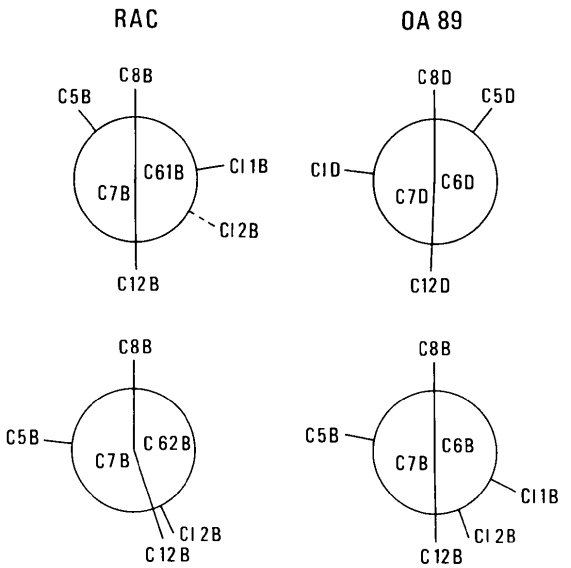

Fig. 2. Newman projections along the C7—C6 bonds of the 3-(2′-chloro-2′-phenylethyl)-2-thiazolidiniminium cations in RAC and OA89.

Table 4. *Bond distances* (Å), *and bond and selected torsion angles* (°) *in the different* 3-(2′-*chloro*-2′-*phenylethyl*)-2-*thiazolidiniminium cations*

RAC		OA89		OA89	
S*B*—C1*B*	1.742 (3)	S*B*—C1*B*	1.740 (4)	S*D*—C1*D*	1.746 (4)
S*B*—C4*B*	1.808 (3)	S*B*—C4*B*	1.813 (6)	S*D*—C4*D*	1.816 (5)
Cl1*B*—C61*B*	1.824 (5)	Cl1*B*—C6*B*	1.464 (14)	Cl*D*—C6*D*	1.831 (5)
Cl2*B*—C62*B*	1.77 (2)	Cl2*B*—C6*B*	1.793 (5)		
N2*B*—C1*B*	1.320 (3)	N2*B*—C1*B*	1.307 (6)	N2*D*—C1*D*	1.323 (6)
N2*B*—C3*B*	1.474 (4)	N2*B*—C3*B*	1.468 (6)	N2*D*—C3*D*	1.465 (5)
N2*B*—C5*B*	1.462 (3)	N2*B*—C5*B*	1.471 (5)	N2*D*—C5*D*	1.466 (5)
N15*B*—C1*B*	1.308 (4)	N15*B*—C1*B*	1.325 (6)	N15*D*—C1*D*	1.301 (6)
C3*B*—C4*B*	1.513 (4)	C3*B*—C4*B*	1.490 (7)	C3*D*—C4*D*	1.515 (6)
C5*B*—C62*B*	1.48 (2)	C5*B*—C6*B*	1.531 (6)	C5*D*—C6*D*	1.523 (5)
C5*B*—C61*B*	1.519 (5)				
C61*B*—C7*B*	1.491 (5)	C6*B*—C7*B*	1.525 (6)	C6*D*—C7*D*	1.498 (5)
C62*B*—C7*B*	1.70 (2)				
C7*B*—C8*B*	1.399 (5)	C7*B*—C8*B*	1.378 (7)	C7*D*—C12*D*	1.378 (6)
C7*B*—C12*B*	1.388 (5)	C7*B*—C12*B*	1.390 (7)	C7*D*—C8*D*	1.395 (7)
C8*B*—C9*B*	1.388 (4)	C8*B*—C9*B*	1.384 (7)	C8*D*—C9*D*	1.381 (6)
C9*B*—C10*B*	1.372 (5)	C9*B*—C10*B*	1.387 (8)	C9*D*—C10*D*	1.386 (7)
C10*B*—C11*B*	1.378 (6)	C10*B*—C11*B*	1.363 (9)	C10*D*—C11*D*	1.370 (8)
C11*B*—C12*B*	1.386 (5)	C11*B*—C12*B*	1.395 (7)	C11*D*—C12*D*	1.402 (6)
C1*B*—S*B*—C4*B*	91.47 (13)	C1*B*—S*B*—C4*B*	91.1 (2)	C1*D*—S*D*—C4*D*	91.6 (2)
C1*B*—N2*B*—C3*B*	115.9 (2)	C1*B*—N2*B*—C3*B*	115.6 (4)	C1*D*—N2*D*—C3*D*	115.3 (3)
C1*B*—N2*B*—C5*B*	125.1 (2)	C1*B*—N2*B*—C5*B*	124.5 (4)	C1*D*—N2*D*—C5*D*	124.4 (4)
C3*B*—N2*B*—C5*B*	118.3 (2)	C3*B*—N2*B*—C5*B*	119.7 (4)	C3*D*—N2*D*—C5*D*	119.8 (3)
N15*B*—C1*B*—N2*B*	126.3 (2)	N15*B*—C1*B*—N2*B*	126.2 (4)	N15*D*—C1*D*—N2*D*	127.1 (4)
N15*B*—C1*B*—S*B*	120.2 (2)	N15*B*—C1*B*—S*B*	119.7 (3)	N15*D*—C1*D*—S*D*	119.7 (3)
N2*B*—C1*B*—S*B*	113.5 (2)	N2*B*—C1*B*—S*B*	114.1 (3)	N2*D*—C1*D*—S*D*	113.1 (3)
N2*B*—C3*B*—C4*B*	106.8 (2)	N2*B*—C3*B*—C4*B*	107.9 (4)	N2*D*—C3*D*—C4*D*	107.5 (3)
C3*B*—C4*B*—S*B*	107.0 (2)	C3*B*—C4*B*—S*B*	107.6 (3)	C3*D*—C4*D*—S*D*	105.4 (3)
N2*B*—C5*B*—C62*B*	110.2 (6)	N2*B*—C5*B*—C6*B*	113.0 (4)	N2*D*—C5*D*—C6*D*	112.5 (3)
N2*B*—C5*B*—C61*B*	113.6 (3)				
C5*B*—C61*B*—C7*B*	114.6 (3)	C5*B*—C6*B*—C7*B*	109.5 (4)	C5*D*—C6*D*—C7*D*	114.4 (3)
C5*B*—C62*B*—C7*B*	105.2 (9)				
C5*B*—C61*B*—Cl1*B*	109.0 (3)	C5*B*—C6*B*—Cl1*B*	136.9 (7)	C5*D*—C6*D*—Cl*D*	107.9 (3)
C5*B*—C62*B*—Cl2*B*	112.6 (10)	C5*B*—C6*B*—Cl2*B*	109.2 (4)		
C7*B*—C61*B*—Cl1*B*	107.9 (3)	C7*B*—C6*B*—Cl1*B*	110.3 (6)	C7*D*—C6*D*—Cl*D*	109.7 (3)
C7*B*—C62*B*—Cl2*B*	109.8 (11)	C7*B*—C6*B*—Cl2*B*	112.1 (3)		
C8*B*—C7*B*—C12*B*	119.4 (3)	C8*B*—C7*B*—C12*B*	119.0 (4)	C8*D*—C7*D*—C12*D*	120.2 (4)
C8*B*—C7*B*—C61*B*	124.0 (3)	C8*B*—C7*B*—C6*B*	116.8 (4)	C8*D*—C7*D*—C6*D*	121.6 (4)
C8*B*—C7*B*—C62*B*	102.2 (7)				
C12*B*—C7*B*—C61*B*	116.6 (3)	C12*B*—C7*B*—C6*B*	124.2 (5)	C12*D*—C7*D*—C6*D*	118.2 (4)
C12*B*—C7*B*—C62*B*	136.3 (7)				
C7*B*—C8*B*—C9*B*	119.8 (3)	C7*B*—C8*B*—C9*B*	121.1 (5)	C7*D*—C8*D*—C9*D*	118.9 (4)
C7*B*—C12*B*—C11*B*	120.1 (3)	C7*B*—C12*B*—C11*B*	119.9 (5)	C7*D*—C12*D*—C11*D*	120.1 (5)
C8*B*—C9*B*—C10*B*	120.1 (3)	C8*B*—C9*B*—C10*B*	119.5 (5)	C8*D*—C9*D*—C10*D*	121.1 (5)
C9*B*—C10*B*—C11*B*	120.7 (3)	C9*B*—C10*B*—C11*B*	120.1 (5)	C9*D*—C10*D*—C11*D*	119.9 (4)
C10*B*—C11*B*—C12*B*	119.9 (3)	C10*B*—C11*B*—C12*B*	120.4 (5)	C10*D*—C11*D*—C12*D*	119.7 (4)
C8*B*—C7*B*—C61*B*—C5*B*	−39.4 (5)	C8*B*—C7*B*—C6*B*—C5*B*	−80.2 (6)	C8*D*—C7*D*—C6*D*—C5*D*	38.4 (7)
C8*B*—C7*B*—C62*B*—C5*B*	−84.2 (10)				
C7*B*—C61*B*—C5*B*—N2*B*	175.4 (3)	C7*B*—C6*B*—C5*B*—N2*B*	−168.0 (4)	C7*D*—C6*D*—C5*D*—N2*D*	−177.2 (4)
C7*B*—C62*B*—C5*B*—N2*B*	−158.0 (6)				
C61*B*—C5*B*—N2*B*—C1*B*	−111.2 (4)	C6*B*—C5*B*—N2*B*—C1*B*	−78.1 (6)	C6*D*—C5*D*—N2*D*—C1*D*	114.3 (5)
C62*B*—C5*B*—N2*B*—C1*B*	−81.1 (9)				
C1*B*—N2*B*—C3*B*—C4*B*	−20.1 (4)	C1*B*—N2*B*—C3*B*—C4*B*	18.2 (7)	C1*D*—N2*D*—C3*D*—C4*D*	23.3 (5)
N2*B*—C3*B*—C4*B*—S*B*	23.9 (3)	N2*B*—C3*B*—C4*B*—S*B*	−19.7 (6)	N2*D*—C3*D*—C4*D*—S*D*	−27.4 (4)
C3*B*—C4*B*—S*B*—C1*B*	−18.5 (3)	C3*B*—C4*B*—S*B*—C1*B*	14.0 (4)	C3*D*—C4*D*—S*D*—C1*D*	21.0 (3)
C4*B*—S*B*—C1*B*—N2*B*	7.9 (2)	C4*B*—S*B*—C1*B*—N2*B*	−4.3 (4)	C4*D*—S*D*—C1*D*—N2*D*	−9.1 (3)
S*B*—C1*B*—N2*B*—C3*B*	6.2 (3)	S*B*—C1*B*—N2*B*—C3*B*	−7.5 (6)	S*D*—C1*D*—N2*D*—C3*D*	−7.0 (5)
N2*B*—C5*B*—C61*B*—Cl1*B*	54.5 (3)	N2*B*—C5*B*—C6*B*—Cl1*B*	−12 (2)	N2*D*—C5*D*—C6*D*—Cl*D*	−54.8 (5)
N2*B*—C5*B*—C62*B*—Cl2*B*	−38.3 (13)	N2*B*—C5*B*—C6*B*—Cl2*B*	−44.9 (5)		
C8*B*—C7*B*—C61*B*—Cl1*B*	82.1 (4)	C8*B*—C7*B*—C6*B*—Cl1*B*	117 (2)	C8*D*—C7*D*—C6*D*—Cl*D*	−83.1 (5)
C8*B*—C7*B*—C62*B*—Cl2*B*	154.3 (8)	C8*B*—C7*B*—C6*B*—Cl2*B*	158.5 (4)		
C12*B*—C7*B*—C61*B*—Cl1*B*	−98.3 (4)	C12*B*—C7*B*—C6*B*—Cl1*B*	−63 (2)	C12*D*—C7*D*—C6*D*—Cl*D*	94.5 (5)
C12*B*—C7*B*—C62*B*—Cl2*B*	−8 (2)	C12*B*—C7*B*—C6*B*—Cl2*B*	−21.8 (7)		

configuration *R*. From this we calculate the ratio of the enantiomers in the crystal to be 0.944 (7)/0.056 (7). As illustrated by the diagrams in Fig. 2, the less populated Cl1*B* atom corresponds to a cation with *S* absolute configuration and a conformation that is twisted by *ca* 30–40° relative to the more abundant geometry. Despite this apparently large variation of the configuration and conformation of the cation, they lead to the same relative positions of the five- and six-membered rings.

Table 5. *Bond distances* (Å), *and bond and selected torsion angles* (°) *in the different p-toluenesulfonate anions*

RAC		OA89		OA89	
S*A*—O2*A*	1.446 (2)	S*A*—O2*A*	1.443 (3)	S*C*—O2*C*	1.444 (3)
S*A*—O3*A*	1.458 (2)	S*A*—O3*A*	1.458 (3)	S*C*—O1*C*	1.457 (4)
S*A*—O1*A*	1.459 (2)	S*A*—O1*A*	1.463 (4)	S*C*—O3*C*	1.459 (3)
S*A*—C1*A*	1.769 (3)	S*A*—C1*A*	1.769 (4)	S*C*—C1*C*	1.768 (4)
C1*A*—C6*A*	1.380 (4)	C1*A*—C6*A*	1.376 (6)	C1*C*—C6*C*	1.385 (6)
C1*A*—C2*A*	1.390 (4)	C1*A*—C2*A*	1.396 (6)	C1*C*—C2*C*	1.386 (5)
C2*A*—C3*A*	1.389 (4)	C2*A*—C3*A*	1.381 (6)	C2*C*—C3*C*	1.391 (5)
C3*A*—C4*A*	1.397 (4)	C3*A*—C4*A*	1.398 (6)	C3*C*—C4*C*	1.392 (6)
C4*A*—C5*A*	1.388 (4)	C4*A*—C5*A*	1.386 (6)	C4*C*—C5*C*	1.387 (6)
C4*A*—C7*A*	1.502 (4)	C4*A*—C7*A*	1.494 (5)	C4*C*—C7*C*	1.516 (5)
C5*A*—C6*A*	1.389 (4)	C5*A*—C6*A*	1.398 (6)	C5*C*—C6*C*	1.389 (6)
O2*A*—S*A*—O3*A*	112.85 (13)	O2*A*—S*A*—O3*A*	113.3 (2)	O2*C*—S*C*—O1*C*	113.1 (2)
O2*A*—S*A*—O1*A*	113.38 (13)	O2*A*—S*A*—O1*A*	112.8 (2)	O2*C*—S*C*—O3*C*	112.6 (2)
O3*A*—S*A*—O1*A*	111.80 (14)	O3*A*—S*A*—O1*A*	111.7 (2)	O1*C*—S*C*—O3*C*	112.1 (2)
O2*A*—S*A*—C1*A*	107.73 (13)	O2*A*—S*A*—C1*A*	107.8 (2)	O2*C*—S*C*—C1*C*	108.0 (2)
O3*A*—S*A*—C1*A*	104.98 (12)	O3*A*—S*A*—C1*A*	105.5 (2)	O1*C*—S*C*—C1*C*	105.2 (2)
O1*A*—S*A*—C1*A*	105.34 (12)	O1*A*—S*A*—C1*A*	105.0 (2)	O3*C*—S*C*—C1*C*	105.1 (2)
C6*A*—C1*A*—C2*A*	120.4 (2)	C6*A*—C1*A*—C2*A*	120.3 (4)	C6*C*—C1*C*—C2*C*	120.1 (4)
C6*A*—C1*A*—S*A*	120.3 (2)	C6*A*—C1*A*—S*A*	120.5 (3)	C6*C*—C1*C*—S*C*	119.9 (3)
C2*A*—C1*A*—S*A*	119.3 (2)	C2*A*—C1*A*—S*A*	119.2 (3)	C2*C*—C1*C*—S*C*	119.9 (3)
C3*A*—C2*A*—C1*A*	119.4 (2)	C3*A*—C2*A*—C1*A*	119.7 (4)	C1*C*—C2*C*—C3*C*	120.0 (4)
C2*A*—C3*A*—C4*A*	121.1 (3)	C2*A*—C3*A*—C4*A*	121.4 (4)	C2*C*—C3*C*—C4*C*	120.5 (4)
C5*A*—C4*A*—C3*A*	118.1 (2)	C5*A*—C4*A*—C3*A*	117.5 (4)	C5*C*—C4*C*—C3*C*	118.5 (4)
C5*A*—C4*A*—C7*A*	120.2 (3)	C5*A*—C4*A*—C7*A*	121.9 (4)	C5*C*—C4*C*—C7*C*	120.3 (4)
C3*A*—C4*A*—C7*A*	121.7 (3)	C3*A*—C4*A*—C7*A*	120.6 (4)	C3*C*—C4*C*—C7*C*	121.2 (4)
C4*A*—C5*A*—C6*A*	121.5 (3)	C4*A*—C5*A*—C6*A*	122.1 (4)	C4*C*—C5*C*—C6*C*	121.4 (4)
C1*A*—C6*A*—C5*A*	119.5 (3)	C1*A*—C6*A*—C5*A*	119.0 (4)	C1*C*—C6*C*—C5*C*	119.4 (4)
O1*A*—S*A*—C1*A*—C2*A*	−56.3 (2)	O1*A*—S*A*—C1*A*—C2*A*	−51.8 (4)	O1*C*—S*C*—C1*C*—C2*C*	56.1 (4)

The most reliable picture of the molecular geometry of the cation is obtained by inspection of the bond lengths and angles for cation *D* (Table 4) in the optically active salt, as this is the only cation not affected by disorder. Within experimental error, the more populated cation at site *B* has similar bond lengths and angles.

The difference between the two C—S distances reflects the sp^2 and sp^3 character of the C1 and C4 atoms, respectively. The C1*D*—N15*D* and C1*D*—N2*D* distances are very short and equal in magnitude, 1.301 (6) and 1.323 (6) Å, respectively. The similarity in the C—N bond lengths and the almost planar arrangement of the S, C1, N15, N2 moiety are consistent with the two equally important resonance formula shown below. The remaining part of the thiazolidine ring is puckered, as illustrated by the torsion angles C1*D*—N2*D*—C3*D*—C4*D* = 23.3 (5) and N2*D*—C3*D*—C4*D*—S*D* = −27.4 (4)°.

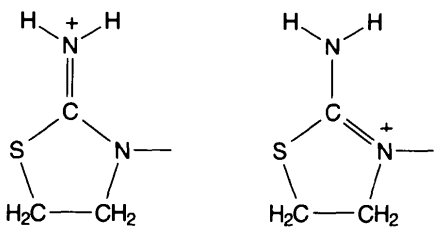

Description of the anion

Almost exact inversion symmetry relates the two *p*-toluenesulfonate ions in the optically active salt; as shown in Table 5, the two O1—S—C1—C2 torsion angles differ by only 4.3 (4)°. Within experimental error, the values are identical to the anion in the racemic salt. The numbering scheme and conformation of the anion are illustrated in Fig. 3. Small variations in the S—O distances are caused by hydrogen bonding (Table 5). O2, which is not involved in any hydrogen bonds, has the shortest S—O2 distance, 1.446 (2) Å.

Comparison of the crystal packing

The similarities between the unit-cell dimensions (Table 1) for 3-(2′-chloro-2′-phenylethyl)-2-thiazolidiniminium *p*-toluenesulfonate of different optical

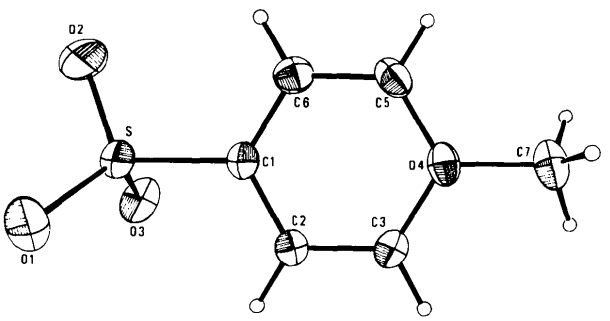

Fig. 3. *ORTEP*II (Johnson, 1976) drawings showing the molecular geometry and numbering scheme of the *p*-toluenesulfonate anion. The thermal ellipsoids are scaled to include 50% probability; H atoms are drawn as spheres with fixed radius.

Table 6 *Hydrogen bonds D—H···A in the different 3-(2′-chloro-2′-phenylethyl)-2-thiazolidiniminium p-toluenesulfonate*

	D···*A* (Å)	*D*—H···*A* (°)	H···*A* (Å)
RAC			
N15*B*—H1N*B*···O1*A*	2.773 (3)	163.48 (9)	1.918 (3)
N15*B*—H2N*B*···O3*A*^{i}	2.751 (3)	168.10 (9)	1.884 (3)
OA89			
N15*B*—H1N*B*···O1*A*	2.771 (5)	161.0 (2)	1.924 (5)
N15*B*—H2N*B*···O3*C*	2.749 (5)	162.78 (14)	1.896 (5)
N15*D*—H1N*D*···O1*C*	2.774 (5)	164.6 (2)	1.916 (5)
N15*D*—H2N*D*···O3*A*	2.743 (5)	170.3 (2)	1.872 (5)

Symmetry code: (i) $1-x, 1-y, 1-z$.

purity have their origin in an almost identical packing of the racemic and the optically active salts.

The crystal packing is dominated by the hydrogen bonds that link the cations and anions. As shown in Table 6, the two protons of the iminium group hydrogen bond to two different *p*-toluenesulfonate ions. In the racemate, the two anions are related by a crystallographic inversion center, in the optically active salt the two independent anions are related by the pseudoinversion center. The hydrogen bonds connect two cations and two anions to form 12-membered rings. The stereo pairs in Figs. 4 and 5 illustrate the packing in the racemic and optically active salts. At a first glance, the two packing diagrams look identical. It requires careful inspection to see that they actually differ with respect to the position of the Cl atom.

DSC measurements were carried out on samples of 3-(2′-chloro-2′-phenylethyl)-2-thiazolidiniminium *p*-toluenesulfonate of different optical purity. The DSC traces did not give any evidence for the existence of an eutectic composition in the phase diagram, thus the compound forms a solid solution (Jacques, Collet & Wilen, 1981). The exact melting points could not be determined because the thermogravimetric measurement showed that the salt decomposes while melting; m.p. 464–466 K for $[\alpha]_D = -25.2$ ($c = 1$, methanol), 467–470 K for racemate. The optically active and racemic salts also had identical FT-IR spectra. The existence of 3-(2′-chloro-2′-phenylethyl)-2-thiazolidiniminium *p*-toluenesulfonate as a solid solution that contains the enantiomers of the cation in all ratios is consistent with the observation that the optical purity does not increase by recrystallization. Although such a mixed crystalline system has been postulated and classified many years ago by Roozeboom (1891, 1899), very few systems have been characterized structurally. Carvoxime is an equivalent example. The structure was determined for a crystal with a composition close to racemic (Baert, Fouret, Oonk & Kroon, 1978) and was compared with the structure of the racemate (Baert & Fouret, 1975; Oonk & Kroon, 1976) and the enantiomer (Kroon, van Gurp, Oonk, Baert & Fouret, 1976).

Racemic carvoxime has an ordered structure and a maximum in the phase diagram corresponding to the racemic composition, which makes it a **true** racemate. Conversely, the racemate of 3-(2′-chloro-2′-phenylethyl)-2-thiazolidiniminium *p*-toluenesulfonate has a disordered structure and displays no obvious maximum in the phase diagram, so it can be classified as a **pseudo**racemate.

Comparison of crystal structures of racemates and enantiomers

The virtually identical crystal packing of the racemic and enantiomeric salts subject to the present investigation raised the following question: Is it a rare incident or does it occur frequently? Pedone &

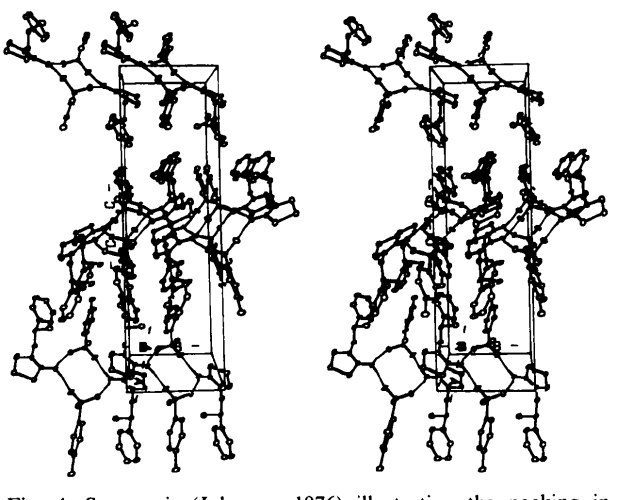

Fig. 4. Stereopair (Johnson, 1976) illustrating the packing in RAC, seen along the *a*-axis. Hydrogen bonds are shown as thin lines.

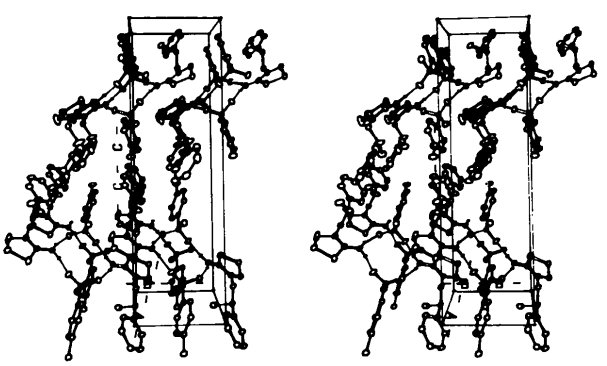

Fig. 5. Stereopair (Johnson, 1976) illustrating the packing in OA89, seen along the *a*-axis. The hydrogen bonds are shown as thin lines. Molecules labelled *A* and *D* are drawn with open bonds.

Table 7. *Pairs of structures for a racemate and the corresponding enantiomer*

REFCODE	Crystal system	Space group	Z	a (Å)	b (Å)	c (Å)	α (°)	β (°)	γ (°)	Hydrogen bonds*
ZEGGIB	Triclinic	$P\bar{1}$	2	9.300 (2)	15.283 (3)	7.808 (1)	96.61 (1)	101.25 (1)	111.12 (1)	+ *R*
ZEGGEX	Triclinic	$P1$	2	9.313 (3)	15.564 (5)	7.764 (2)	96.76 (2)	102.03 (3)	111.80 (3)	+ *R*
BAGMUR	Monoclinic	$P2_1/n$	4	15.824 (3)	12.704 (1)	9.559 (1)		92.78 (2)		+ *R*
BAGMOL	Monoclinic	$P2_1$	4	16.036 (3)	12.606 (1)	9.634 (1)		94.44 (2)		+ *R*
COBDEC	Monoclinic	$P2_1/a$	4	8.691 (10)	28.05 (2)	8.864 (7)		114.49 (7)		*R*
COBDEC	Monoclinic	$P2_1$	4	8.875 (7)	28.525 (10)	8.695 (5)		115.59 (6)		*R*
BZPPBA	Monoclinic	$P2_1/c$	4	9.206 (3)	10.530 (4)	17.223 (5)		111.89 (6)		+
EBPVPO	Monoclinic	$P2_1$	4	9.147 (3)	10.294 (3)	16.911 (4)		98.08 (4)		+
CARVOX	Monoclinic	$P2_1/c$	4	9.856 (3)	11.848 (3)	8.480 (3)		98.95 (5)		+
LCARVX	Monoclinic	$P2_1$	4	10.24 (1)	11.67 (1)	8.54 (2)		103.1 (1)		+
PRCOUM	Monoclinic	$P2_1/n$	4	11.407 (3)	18.005 (4)	7.177 (2)		95.30 (10)		+
PPRHCM†	Monoclinic	$P2_1$	4	11.752 (2)	17.751 (5)	7.171 (1)		92.58 (2)		+
KUHLAA‡	Monoclinic	$P2_1/c$	4	7.349 (1)	7.203 (2)	24.729 (4)		91.27 (1)		
KUHLEE‡	Orthorhombic	$P2_12_12_1$	4	7.3342 (8)	7.3587 (4)	24.613 (6)				
DLALNI	Orthorhombic	$Pna2_1$	4	12.06 (1)	6.05 (1)	5.82 (1)				+
LALNIN†	Orthorhombic	$P2_12_12_1$	4	12.343 (1)	6.032 (1)	5.784 (1)				+
DLTYRS	Orthorhombic	$Pna2_1$	4	20.8360 (8)	6.810 (2)	5.905 (1)				+
LTYROS†	Orthorhombic	$P2_12_12_1$	4	21.116 (3)	6.913 (5)	5.829 (4)				+
MBABIQ	Orthorhombic	$Pna2_1$	4	8.571 (4)	30.754 (2)	5.957 (2)				+
MBABIQ	Orthorhombic	$P2_12_12_1$	4	8.730 (5)	30.094 (4)	5.950 (2)				+
FBPACR†	Orthorhombic	$Pc2_1n$	4	5.95 (1)	7.66 (1)	19.25 (3)				+
DFBPAC	Monoclinic	$P2_1$	2	5.963 (5)	7.411 (6)	10.019 (9)		102.9 (1)		+
APALAM	Monoclinic	$P2_1/n$	4	19.45 (4)	4.98 (1)	12.29 (2)		91.92 (7)		+
APHAMA†	Monoclinic	$P2_1$	2	11.531 (1)	4.966 (1)	11.695 (1)		116.6 (1)		+
CDBMPI	Monoclinic	$P2_1/a$	4	11.220 (6)	14.571 (6)	10.688 (7)		99.38 (8)		
BZMPIZ†	Monoclinic	$P2_1$	2	5.889 (5)	14.251 (12)	10.789 (7)		102.59 (6)		
DLVALC	Monoclinic	$P2_1/c$	4	11.722 (4)	7.007 (3)	11.143 (4)		120.53		+
VALEHC	Monoclinic	$P2_1$	2	10.382 (2)	7.066 (1)	5.4407 (9)		91.40 (2)		+

* Hydrogen bonds observed in the structure; *R* the racemate is prepared by X-ray exposure.
† The axes are permuted to show the similarities.
‡ Entitled Thioph6 in Brock, Schweitzer & Dunitz (1991).

Benedetti (1972) gave three examples of identical packing for a racemate and the corresponding enantiomer. Since no systematic structural comparison has been performed previously for racemates and corresponding enantiomers, it was a natural extension of the present investigation to perform such an analysis, making use of the information in the Cambridge Structural Database (CSD) (Allen, Kennard & Taylor, 1983).

Brock, Schweitzer & Dunitz (1991) compared the density of racemic crystals with their chiral counterparts, using extracted structural information from the CSD. They classified the structures into two groups, one which contains the enantiomers that readily racemize and the other with resolvable enantiomers. We have used the latter group of structures as a basis for our investigations. From this group Brock, Schweitzer & Dunitz (1991) excluded entries lacking coordinates, crystallographic *R*-values larger than 0.15 and structures that were marked as suffering from errors of disorder. Thus, we may have excluded structures that resemble those of the present study. The resulting 64 structures were analysed for similarities between crystal structures of the racemate and the corresponding enantiomer. A comparison of the cell dimensions with special emphasis on unique axes was made first. Equivalent symmetry operations were also sought in the space groups for a racemate and the corresponding enantiomer. The overall packing was checked on a graphics system (Insight II, 1992).

We found a large diversity in the relations between the structures of a racemate and the corresponding enantiomer ranging from identical to completely different packing modes. According to the degree of similarity, the 14 pairs listed in Table 7 have been classified into three groups. For the first group, the racemate and the enantiomer have the same number

of molecules in the unit cells of almost identical dimensions. In these cases, the enantiomer structure has two independent molecules in the asymmetric unit that interact in a mode identical to that found in the racemate structure, just as observed for the compound we investigated. As shown in Table 7, an additional pseudoinversion center relates the two independent molecules in all six enantiomeric structures. It must be noted that half the examples in this group are structures where the racemate is formed by a photochemically induced solid-state reaction of cobaloxime complexes. One cannot exclude that this could favor the formation of a metastable form of the racemate. The packing in the other structures in this group is strongly influenced by hydrogen bonds.

The unit-cell dimensions are also very similar in the second group of structures, which contains four racemate/enantiomer pairs. All the structures have one independent molecule per asymmetric unit. Three of the racemate/enantiomer pairs crystallize in the space groups $Pna2_1$ and $P2_12_12_1$. The relative positions of the symmetry elements are the same in these two space groups. Both the racemate and the enantiomer structures contain layers of identical chirality and differ only in their interlayer interactions.

The last group consists of four pairs of structures in which two of the lattice periods are identical for the racemate and the enantiomer. In the third direction, the axis of the enantioner is half that of the racemate. All the enantiomeric structures in this group crystallize in the space group $P2_1$. The relative position of the two molecules of identical chirality in the enantiomeric structure is preserved in the structure of the racemate. The racemate/enantiomer structures differ only in the direction where the enantiomer is half the size of the racemate. In this direction, the molecules are related by translational symmetry in the structure of the enantiomer and by the symmetry of a glide plane (inversion center) in the racemate structure. This relation has been described earlier by Di Blasio, Napolitano & Pedone (1977) in their analysis of the structures of racemic and optically active valine hydrochloride.

The present comparison has revealed that identical packing in structures of a racemate and the corresponding enantiomer cannot be called a rare incident. The racemate and the corresponding enantiomer contain identical functional groups with the possibility of forming identical hydrogen bonds, therefore, it is not surprising that the similarity between racemates and the corresponding enantiomers appears to be more pronounced in systems where the packing is influenced by hydrogen bonding.

We thank Mr Flemming Hansen for help with the crystallographic experiments and Dr Izvekov Vladislav for recording the IR spectra. The thermoanalytical equipment was made available through a grant from the Lundbeck Foundation. The research was supported financially by OTKA grant T-4183 and by grants from the Varga József Foundation, the Danish Natural Science Research Council and the Danish Research Academy. The latter institution financed Katalin Marthi's stay in Denmark.

References

ALLEN, F. H., KENNARD, O. & TAYLOR, R. (1983). *Acc. Chem. Res.* **16**, 146–153.

BAERT, F. & FOURET, R. (1975). *Cryst. Struct. Commun.* **4**, 307–310.

BAERT, F., FOURET, R., OONK, H. A. J. & KROON, J. (1978). *Acta Cryst.* B**34**, 222–226.

BLESSING, R. (1987). *Cryst. Rev.* **1**, 3–58.

BROCK, C. P., SCHWEITZER, W. B. & DUNITZ, J. D. (1991). *J. Am. Chem. Soc.* **113**, 9811–9820.

DI BLASIO, B., NAPOLITANO, G. & PEDONE, C. (1977). *Acta Cryst.* B**33**, 542–545.

FLACK, H. D. (1983). *Acta Cryst.* A**39**, 876–881.

FLACK, H. D. & SCHWARZENBACH, D. (1988). *Acta Cryst.* A**44**, 499–506.

InsightII (1992). *Reference Guide*, Version 2.1.0. Biosym Technologies, San Diego, USA.

JACQUES, J., COLLET, A. & WILEN, S. H. (1981). *Enantiomers, Racemates, and Resolutions*, pp. 104–131. New York: Wiley.

JOHNSON, C. K. (1976). *ORTEP*II. Report ORNL-5138. Oak Ridge National Laboratory, Tennessee, USA.

KROON, J., VAN GURP, P. R. E., OONK, H. A. J., BAERT, F. & FOURET, R. (1976). *Acta Cryst.* B**32**, 2561–2564.

NEGWER, M. (1978). (Editor). *Organic-Chemical Drugs and their Synonyms*, Vol. 1, p. 288. Berlin: Academie Verlag.

OONK, H. A. J. & KROON, J. (1976). *Acta Cryst.* B**32**, 500–504.

PEDONE, C. & BENEDETTI, E. (1972). *Acta Cryst.* B**28**, 1970–1971.

ROOZEBOOM, H. W. B. (1891). *Z. Phys. Chem.* **8**, 504–530.

ROOZEBOOM, H. W. B. (1899). *Z. Phys. Chem.* **28**, 494–517.

SHELDRICK, G. M. (1990). *Acta Cryst.* A**46**, 467–473.

SHELDRICK, G. M. (1995). *J. Appl. Cryst.* In preparation.

SPICER, L. D., BULLOCK, M. W., GARBER, M., GROTH, W., HAND, J. J., LONG, D. W., SAWYER, J. L. & WAYNE, R. S. (1968). *J. Org. Chem.* **33**, 1350–1353.